

05,11

First Order Phase Transition in Ferromagnetic Semiconductors in External Electric and Magnetic Fields (by the example of $\text{La}_{1-x}\text{Ca}_x\text{MnO}_3$) (on the example of $\text{La}_{1-x}\text{Ca}_x\text{MnO}_3$)

© A.A. Povzner, A.G. Volkov, E.I. Lopatko, N.A. Zaitseva

Ural Federal University after the first President of Russia B.N. Yeltsin,
Yekaterinburg, Russia

E-mail: a.a.povzner@urfu.ru

Received December 15, 2022

Revised February 8, 2023

Accepted February 9, 2023

It is shown that during a first-order phase transition in ferromagnetic semiconductors based on lanthanum manganites, along with the semiconductor phase of s-electrons, a phase arises with fluctuation short-range order associated with a change in the sign of the intermode interaction parameter in the system of d-electrons. The phase separation region is characterized by fluctuations of local magnetization depending on temperature and external magnetic field. In this case, the temperature of the first order phase transition, above which phase separation arises, is appreciably affected by double exchange. Due to self-heating, the phase separation is significantly affected by the electric field, which leads to N-shaped current-voltage characteristics. Using $\text{La}_{1-x}\text{Ca}_x\text{MnO}_3$ as an example, it is shown that the switching on of electric and magnetic fields during a first-order phase transition in ferromagnetic semiconductors is accompanied by the appearance of self-oscillations of the electric current and magnetization.

Keywords: double exchange, electron fluctuations of spin and charge density, Anderson localization, self-oscillations.

DOI: 10.21883/PSS.2023.04.55991.528

1. Introduction

It is well known that in ferromagnetic semiconductors with colossal magnetoresistance (CMR) an abnormally strong bond between spin and electron subsystems is implemented, which leads to the Anderson localization of conduction electrons in case of magnetic phase transition and to the metal–insulator electronic transition [1]. However, microscopic nature of the magnetic phase transition in the group of ferromagnetic semiconductors in question, for example, in lanthanum manganites, is not finally established.

It is recognized that the main cause of ferromagnetism in this group is the double exchange arising due to the intra-atomic Hund interaction of conduction s-electrons with d-electrons that are believed to be localized [2]. However, it is known that in the system of d-electrons of ferromagnetic metals and compounds a competition arises between their intra-atomic Coulomb interaction and their band motion [3,4]. Therefore, the model of double exchange in ferromagnetic semiconductors with CMR should be added with accounting of correlations in the system of d-electrons.

In addition, to describe band motion of s-electrons and d-electrons in specific compounds of ferromagnetic semiconductors with CMR, ab initio DFT-calculations of their electron spectra and densities of electron states (DoS) are needed. At the same time, it is worth to note that the information in databases regarding the electronic structure of the metal ground state of this group of semiconductors [5,6]

shows the presence of topological features of the electron spectrum.

Until recently, the role of topological features of the thin structure of DoS that determine the magnitude and sign of the intermode interaction parameter in the Ginzburg–Landau functional (see, for example, [7]) has not been considered. It is known that from the analysis of this functional it follows that first-order phase transitions, in contrast to second-order phase transitions, are accompanied by a change in sign of the intermode interaction parameter, which takes place between maximum and local minimum of DoS [5,6].

In the case of first-order phase transitions a short-range order with local magnetization is observed in ferromagnetic semiconductors [8]. A feature of phase transitions in ferromagnetic semiconductors is the emergence of strongly nonlinear current-voltage curves in electric field, which are noticeably affected by magnetic field [9,10].

In this context, this study investigates the first-order phase transition in external electric and magnetic fields using the example of $\text{La}_{1-x}\text{Ca}_x\text{MnO}_3$.

2. Model

Let us consider a system of d-electrons with intra-atomic Coulomb correlations and conduction s-electrons¹ intercon-

¹ Both s-electrons and p-electrons are considered as conduction electrons, the later are s-like in this model.

ned by a strong sd-exchange interaction. Hamiltonian of this electron system is as follows

$$H = \sum_{l=s,p,d} H_0^{(l)} + H_{dd} + H_{sd}, \quad (1)$$

where $H_0^{(l)}$ is Hamiltonian of band motion of s ($l = s$)-electrons and d ($l = d$)-electrons, H_{dd} is Hamiltonian of intra-atomic Hubbard (U) and Hund (J_{dd}) interactions of d-electrons, and the Hamiltonian of Hund interaction of s-electrons and d-electrons at a site [2] will be described in the mean field approximation

$$H_{sd} = -J_{sd} \sum_{\nu} \mathbf{S}_{\nu} \mathbf{s}_{\nu} \approx -J_{sd} \sum_{\nu} (\langle \mathbf{S}_{\nu} \rangle \mathbf{s}_{\nu} + \mathbf{S}_{\nu} \langle \mathbf{s}_{\nu} \rangle).$$

Here \mathbf{S}_{ν} and \mathbf{s}_{ν} are spin vector operators of d-electron and s-electron at the site ν .

We reduce the intra-atomic Coulomb correlations in the system of d-electrons to the description of their motion in exchange (ξ) and charge (η) fields fluctuating in space and time [4]. Then, using Hubbard–Stratonovitch transformations (see, for example, [4]) and the technique of Matsubara Green functions [11] (defined on four vectors $q = (\mathbf{q}, \omega_{2n})$, where \mathbf{q} being quasipulse, ω_{2n} being Matsubara Bose frequency), free energy of the electron system can be represented as follows:

$$F = F_0 - T \ln \int (d\xi d\eta) \exp(-\Phi(\xi, \eta)/T). \quad (2)$$

Here

$$F_0 = T \sum_{\mathbf{k}, \sigma, l} \ln(1 + \exp[(\epsilon_{\mathbf{k}, l} - \sigma J_{sd} M_0^{(l)} - \mu)/T]); \quad (3a)$$

$$\begin{aligned} \Phi(\xi, \eta) = & TN_j \sum_q (D_q^{-1} |\xi_q|^2 - (2 - D_q^{-1} + b - a) |\hat{\eta}_q|^2) \\ & + \sum_q (U^{-1} |J_q \mathbf{M}_q^{(s)}|^2 - 2(U/T)^{1/2} N_j J_{-q} (\xi_q \mathbf{M}_{-q}^{(s)})) \\ & + (3!)^{-1} \kappa T N_j \sum_{q_1+q_2+q_3+q_4=0} (\xi_{q_1} \xi_{q_2} \xi_{q_3} \xi_{q_4} - 4 \xi_{q_1} \xi_{q_2} \hat{\eta}_{q_3} \hat{\eta}_{q_4} \\ & + \hat{\eta}_{q_1} \hat{\eta}_{q_2} \hat{\eta}_{q_3} \hat{\eta}_{q_4}) - H(N_j \xi_0^{(z)} + M_0^{(s)}) \end{aligned} \quad (3b)$$

takes into account space-time dependencies of fluctuating fields; T is temperature in energy units; H is modulus of strength vector of the homogeneous external magnetic field directed along the Oz axis, in energy units; N_j is orbital degeneracy of partly occupied energy states of d-electrons; $\hat{\eta}_q = \eta_q (U/T)^{1/2} (2N_j)^{-1} n_d \delta_{q,0}$; n_d is number of d-electrons per site; $\mathbf{M}_q^{(l)}$ is Fourier-image of the local magnetization vector of s-electrons or d-electrons ($l = s$ or d) in $2\mu_B$ units (μ_B is Bohr magneton),

$$D_q = (1 - U\chi_q^{(d)} - J_{sd}^2 \chi_q^{(s)} U^{-1} - a)^{-1}; \quad (4)$$

$J_q = J_{dd}^2 \chi_q^{(s)}$; $\chi_q^{(s)}$ and $\chi_q^{(d)}$ are Pauli susceptibilities of s-electrons and d-electrons;

$$\kappa = 4^{-1} U^3 (g_d^{(2)}(\mu) - (g_d^{(1)}(\mu))^2 / g_d(\mu)) \quad (5)$$

is parameter of intermode interaction; μ is chemical potential; $g_s(\epsilon)$ and $g_d(\epsilon)$ is density of states of s-electrons and d-electrons calculated in the DFT + U-approximation; $g_l^{(n)}(\epsilon) (= d^n g_l(\epsilon) / d\epsilon^n)$; $a = J_{dd} U (U - J_{dd})^{-1} (U + 5J_{dd}^{-1})$ and $b = 4U (U - 5J_{dd})^{-1}$.

To derive magnetic equations of state, functional integrals in (2) are calculated in a saddle point approximation (see [4]) with respect to $r_q = |\xi_q|$, $\varphi_q = \arg(\xi_q)$, ξ_q , ξ_0 , η_q variables. Then, by minimizing the free energy with respect to magnetizations ($\mathbf{M}_q^{(l)}$), taking into account the relation of saddle values to the thermodynamic mean values, the following is derived

$$\begin{aligned} M_{q,\gamma}^{(d)} (D_q^{-1} + 5\kappa \langle \mathbf{m}^2 \rangle / 3) + \kappa \sum_{q_1, q_2, q_3} \hat{\eta}_{q_1} [(\mathbf{M}_{q_2}^{(d)} \mathbf{M}_{q_3}^{(d)}) \\ - 4^{-1} \hat{\eta}_{q_2} \hat{\eta}_{q_3}] \delta_{q_1+q_2+q_3+q_4=0} = \delta_{\gamma,z} (H \delta_{q,0} + J_{sd} M_{q,\gamma}^{(s)}) / U, \end{aligned} \quad (6a)$$

$$M_{q,\gamma}^{(s)} = g_s(\mu) (H \delta_{q,0} \delta_{\gamma,z} + J_H^2 \chi_q^{(s)} M_{q,\gamma}^{(d)}), \quad (6b)$$

$$(2 + a - b - D_q^{-1} - 5\kappa \langle \mathbf{m}^2 \rangle / 3)$$

$$- \kappa \sum_{q_1, q_2, q_3} \hat{\eta}_{q_1} [(\mathbf{M}_{q_2}^{(d)} \mathbf{M}_{q_3}^{(d)}) - 4^{-1} \hat{\eta}_{q_2} \hat{\eta}_{q_3}] \delta_{q_1+q_2+q_3+q_4=0} = 0. \quad (6c)$$

Here H is strength of the magnetic field directed along the Oz axis; $\langle \mathbf{m}^2 \rangle$ is squared amplitude of Bose fluctuations of spin density of d-electrons defined by (see [11]) the fluctuation-dissipation theorem (FDT) with the Bose–Einstein function ($f_B(\omega/T)$):

$$\langle \mathbf{m}^2 \rangle = \sum_q \int_0^{\infty} d\omega f_B(\omega/T) \text{Im} \chi(q, \omega),$$

$f_B(\omega/T)$ is Bose function, where magnetic susceptibility of d-electrons is

$$\begin{aligned} \chi(\mathbf{q}, \omega) = & \chi^{(d)}(\mathbf{q}, \omega) (1 - U\chi^{(d)}(\mathbf{q}, \omega) \\ & + 2\kappa \sum_q |\mathbf{M}_q|^2 + 5\kappa \langle \mathbf{m}^2 \rangle / 3)^{-1}, \end{aligned}$$

with $\chi^{(d)}(\mathbf{q}, \omega) = \chi_0^{(d)} - A\mathbf{q}^2 + iB\omega/|\mathbf{q}|$ according to the known approximation of the Lindhard function [4].

3. Solution to the magnetic equation of state near T_C

Ferromagnetic solutions to magnetic equations of state are derived at $D_0^{-1} < 0$ and $\kappa > 0$. At the same time,

it can be shown that at least near and below the Curie temperature, with

$$|1 - U\chi_0^{(d)} - a + 5\kappa\langle\mathbf{m}^2\rangle/3 + \kappa M_0^{(d)2}| \ll J_{sd}^2\chi_0^{(s)}U^{-1}, \quad (7)$$

the decisive factor for the existence of ferromagnetism is the double sd-exchange.

With $T > T_C$ the mode–mode parameter changes its sign ($\kappa < 0$), ferromagnetism loses its thermodynamic stability and solutions to equation (6) describe the phase of ferromagnetic short-range order with a local magnetization of d-electrons

$$M_{q,\gamma}^{(d)} = \sum_q |M_{q,\gamma}^{(d)}| \exp(iqv + i\varphi_{q,\gamma})$$

and fluctuations of occupation numbers of d-electrons at the site

$$n_v = 2^{-1} \sum_q |\eta_q| \exp(iqv + i\varphi_{q,z}),$$

where $\varphi_{q,\gamma}$ is chaotically changing difference of electronic Berry phases ($\gamma = x, y, z$).

Spatial dimensions of the regions of ferromagnetic short-range order with fixed local magnetization modulus $M_s = \langle\delta\mathbf{M}^2\rangle^{1/2}$ are characterized by the radius of ferromagnetic spin correlations

$$R_C = (2\varepsilon_F/m_{\text{eff}})^{-1} (|\kappa|/\mathbf{A})^{1/2} (M_s^2 + \mathbf{M}_0^2(H))^{-1/2}, \quad (8)$$

where ε_F and m_{eff} are Fermi energy and effective electron mass of d-electrons.

At the same time, the fluctuations of electron density that depend on temperature and external magnetic field are determined by the following equations:

$$\langle\delta\mathbf{M}^2\rangle = \{|\kappa|[(\mathbf{M}_0^2(H) + 5\langle\mathbf{m}^2\rangle/3)(1 + J_{dd}^2/U^2) - \langle\delta n^2\rangle] + A - D_0^{-1}\}/|2\kappa|, \quad (9a)$$

$$\langle\delta n^2\rangle = \{2 - a + b - D_0^{-1} + A - |\kappa|[(\mathbf{M}_0^2(H) + \langle\delta\mathbf{M}^2\rangle + 5\langle\mathbf{m}^2\rangle/3)(1 + J_{dd}^2/U^2)]\}/|\kappa|. \quad (9b)$$

The root-mean-square amplitude of thermal dynamic Bose fluctuations of spin density ($\langle\mathbf{m}^2\rangle$) according to (6) is as follows

$$\langle\mathbf{m}^2\rangle = B(T/U)^2 (|\kappa|(\mathbf{M}_0^2(H) - \langle\delta n^2\rangle + \langle\delta\mathbf{M}^2\rangle) - A)^{-2}$$

and turns to be $(T/U)^2$ times less than the amplitude of spatial static fluctuations (9a).

An important feature of the phase transition under consideration is the emergence of semiconductor phase with the Anderson localization of conduction s-electrons. Due to the sd-exchange, the conduction s-electrons fall into the field of random potential

$$V_v = \sigma \sum_{\mu} J_{\mu,\mu} \delta M_{\mu},$$

where

$$J_{v,\mu} = J_{dd}^2 \sum_q \chi_q^{(s)} \exp\{q(v - \mu)\}.$$

According to [12], it leads to their localization, provided that the chemical potential falls into the energy region between the edge of the band and the energy value that differs from it by a percolation threshold

$$E_C = J_{sd}^2 M_s^2 / \Delta, \quad (10)$$

where Δ is route-mean-square of the integral of conduction electrons hop between neighbor sites in the lattice occupied by manganese atoms.

As a result, the conductivity $\sigma(T)$ changes with temperature following the activation law

$$\sigma(T) = \sigma_0 \exp(-T^{-1}E_A),$$

where E_A is activation energy that will be defined below after calculations of the electronic structure.

The chemical potential of the electron system is determined from the condition of electrical neutrality for the sum concentration of s-electrons and d-electrons:

$$n = n_s + 2N_d \left[\int d\varepsilon f(\varepsilon - \mu) g_d(\varepsilon) + U g_d^{(1)}(\mu) (\langle\mathbf{m}^2\rangle + |\mathbf{M}_0|^2 + \langle\delta\mathbf{M}^2\rangle - \langle\delta\eta^2\rangle) / 4 \right], \quad (11)$$

$$n_s = 2 \int_{-\infty}^{\infty} g_s(\varepsilon) f(\varepsilon - \mu) d\varepsilon,$$

$g_s(\varepsilon)$ is density of states of conduction electrons.

4. Numerical analysis of the phase transition

The calculations of DoS taking into account the crystalline structure of $\text{La}_{1-x}\text{Ca}_x\text{MnO}_3$ were performed on the basis of ab initio DFT-modeling. To describe in a more correct way the spatial inhomogeneities of the distribution of electron density in $\text{La}_{1-x}\text{Ca}_x\text{MnO}_3$ at $x = 0.3$, the GGA + U + SO-calculations of DoS were performed (Fig. 1). Wave functions were selected on a $5 \times 4 \times 5$ grid of k -points and length of the „cut-off“ wave vector was set equal to $4.16 \text{ at. units}^{-1}$. For other ferromagnetic compounds a rigid strip approximation was used.

To analyze thin structure of the $g_d(\varepsilon)$ dependence, the results of GGA + U + SO-calculation were approximated in the energy range of $-0.2 < \varepsilon < 0.4 \text{ eV}$ by the following polynomial:

$$g_d(\varepsilon) = -335.31\varepsilon^8 - 154.77\varepsilon^7 + 147.05\varepsilon^6 + 61.9\varepsilon^5 - 19.90\varepsilon^4 - 6.97\varepsilon^3 + 0.71\varepsilon^2 + 0.18\varepsilon + 0.30, \text{ eV}^{-1}.$$

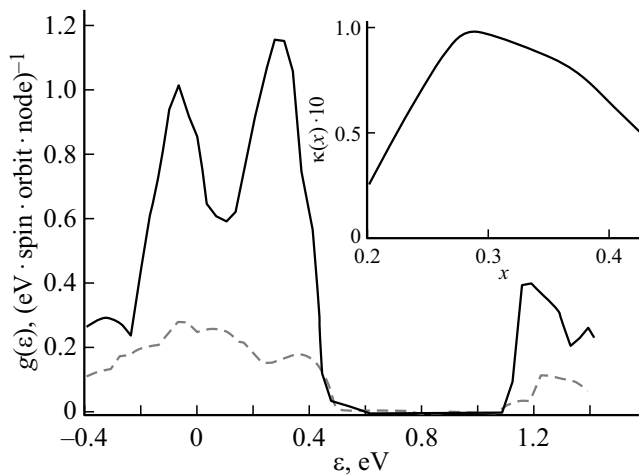


Figure 1. Results of GGA + U + SO-calculations of the function of density of states of d-electrons ($g_d(\varepsilon)$ — solid line) and conduction electrons ($g_s(\varepsilon)$ — dashed line). The origin of energy count coincides with the Fermi energy for $\text{La}_{0.7}\text{Ca}_{0.3}\text{MnO}_3$. In the insert: concentration dependence of the parameter of intermode interaction $\kappa(x)$ at $T = 0\text{ K}$.

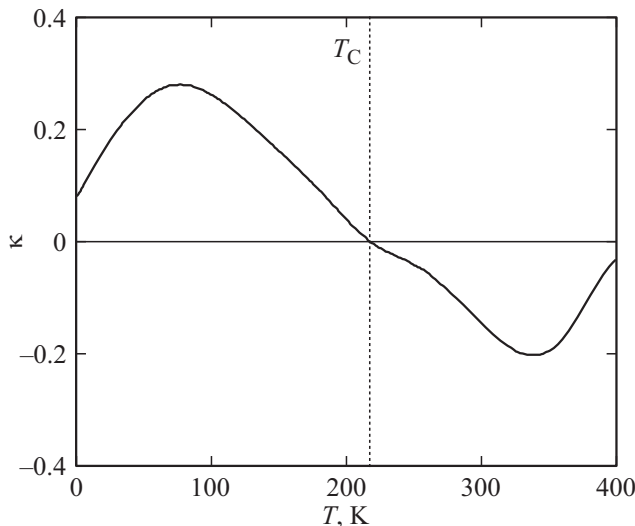


Figure 2. Temperature dependence of the intermode interaction coefficient for $\text{La}_{1-x}\text{Ca}_x\text{MnO}_3$ at $x = 0.3$ and $H = 0$ ($T_C = 218\text{ K}$).

In doing this, a point of inflection was found for the $g_d(\varepsilon)$ dependence where the change in sign of its curvature and the mode–mode parameter takes place.

It was found for $\text{La}_{1-x}\text{Ca}_x\text{MnO}_3$ ferromagnetic compounds that in the range of concentrations from $0.2 < x < 0.45$ the exchange enhancement factors in the ground state are negative, and it was found that the mode–mode parameter in their ground state is positive (insert in Fig. 1). In the entire aforementioned region of concentrations at a temperature of T_C temperature first-order phase transitions are realized. These transitions are accompanied by a change in sign of the intermode interac-

tion parameter (Fig. 2) and an emergence of fluctuations of local magnetization (9a).

Results of calculations of the concentration dependence T_C in comparison with the experimental findings are shown in Fig. 3. It turns out that the consistency with the experimental Curie temperature is achieved at $U = 1.8\text{ eV}$, $J_{sd} = 1.15\text{ eV}$. In this case the parameter of Hund dd-interaction in the Elk software package used in the study (<http://elk.sourceforge.net>) is determined automatically and equal to $J_{dd} = 0.63\text{ eV}$. Orbital degeneracy of the partly occupied d-band is $N_j = 4$.

In addition, direct band calculations show that in the energy region below the energy gap (see Fig. 1) a mixture of t_{2g} and e_g d-states takes place. It means that the spatial charge fluctuations arising in accordance with formula (9b) correspond to fluctuations of the Mn ion valence in the model of electronic structure under consideration.

As it is shown by the evaluations based on formula (9), spatial fluctuations of the local magnetization of d-electrons

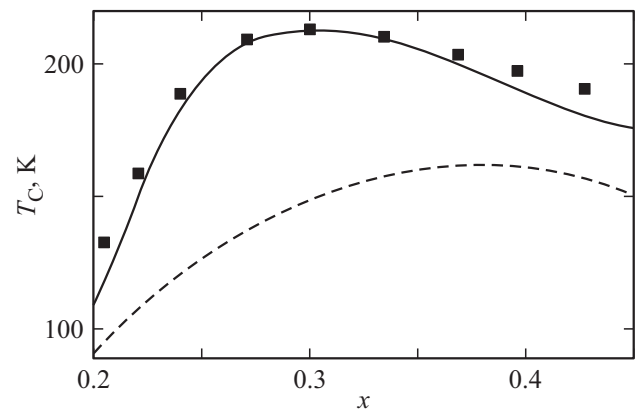


Figure 3. Concentration dependence of Curie temperature for $\text{La}_{1-x}\text{Ca}_x\text{MnO}_3$ in relative units. Solid line and dashed line show the calculation with and without taking into account the double exchange, dots show the experimental result [1].

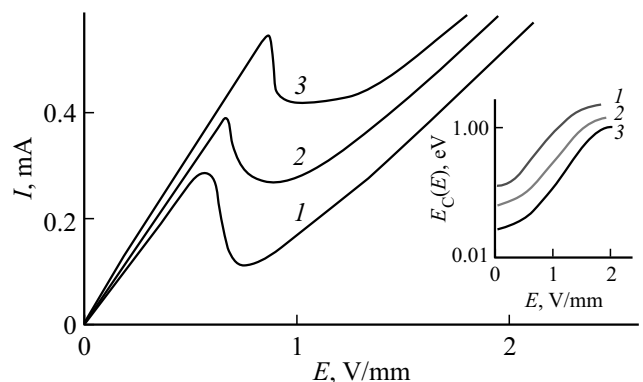


Figure 4. IU-curve of $\text{La}_{0.7}\text{Ca}_{0.3}\text{MnO}_3$ samples with a size of $1 \times 1 \times 0.01\text{ mm}^3$ at $T_0 = 220\text{ K}$, $\lambda = 15\text{ W}/(\text{m}^2 \cdot \text{K})$ (as in [14]) at the following inductions of the magnetic field: 0 (curve 1), 3 (curve 2), 5 T (curve 3). In the insert: percolation threshold as a function of electric field strength in different magnetic fields.

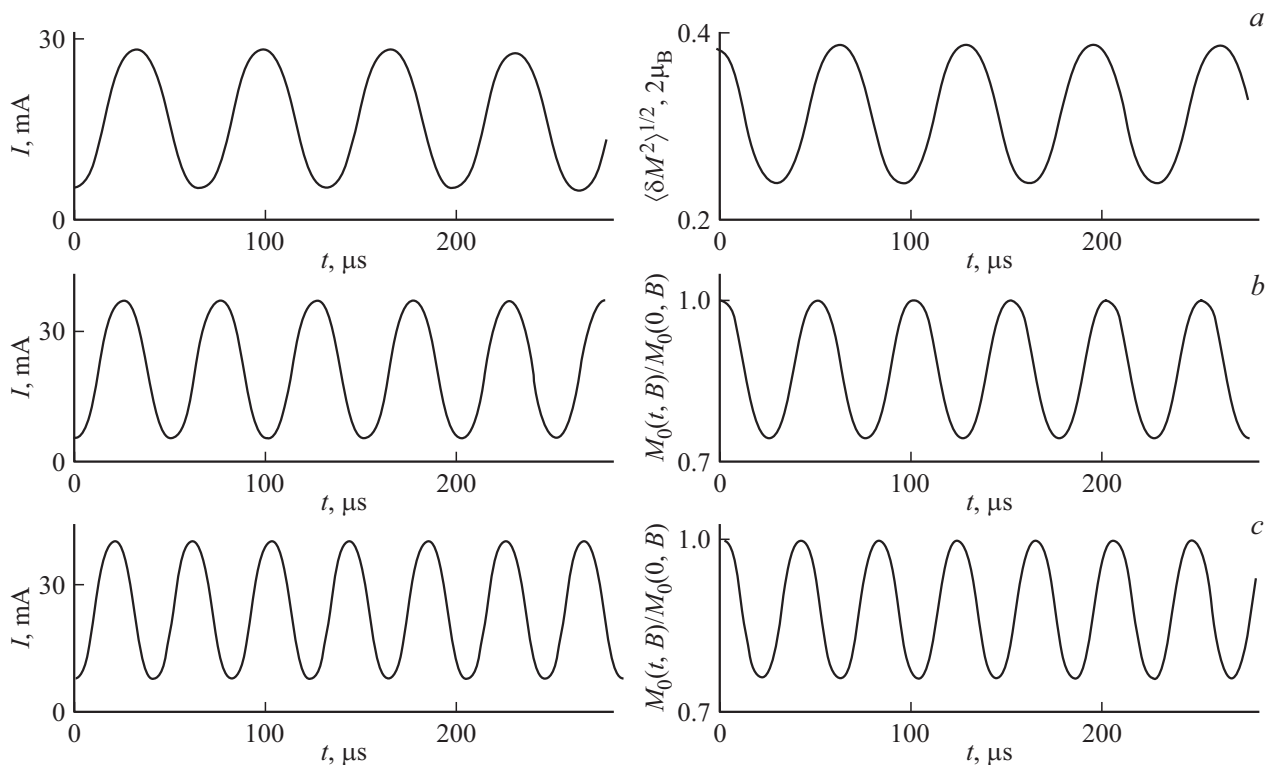


Figure 5. Self-oscillations of current I , root-mean-square amplitude of fluctuations of local magnetization (at $B = 0$ T) and magnetization (in an external magnetic field) for the $\text{La}_{0.7}\text{Ca}_{0.3}\text{MnO}_3$ sample with a size of $1 \times 1 \times 0.01 \text{ mm}^3$. Here $T_0 = 220 \text{ K}$ and $E = 0.3 \text{ kV/m}$, $M_0(0, 0) \approx 0.1 \mu_B$. Frequencies in figures: a) $B = 0$ T, $\nu = 15 \text{ kHz}$; b) $B = 3$ T, $\nu = 20 \text{ kHz}$; c) $B = 5$ T, $\nu = 25 \text{ kHz}$.

give values of about 10 lattice constants for the ferromagnetic compounds in question. And the decisive contribution to the formation of the temperature dependence of electric conductivity is made by the semiconductor phase of s-electrons.

Numerical analysis of the electronic structure shows that the semiconductor phase of Anderson-localized conduction s-electrons arising with the phase immiscibility is realized under the condition that the chemical potential is near the band gap. In this case the energy of activation is $E_A = (E_C - \varepsilon_c + \mu)$, where ε_c is energy of the top edge of the partly occupied d-band.

Evaluations of the activation conductivity dependence on temperature and external magnetic field, carried out with consideration of formulae (9,10) are consistent with the CMR effect observed in the considered compounds. At the same time, the performed numerical analysis shows that the strong influence of magnetic field follows from formulae (9) for spatial fluctuations of electron density.

5. Phase transition in external electric and magnetic fields

In external electric fields (E) a current of conduction electrons arises with a density of $j(T) \approx \exp(-T^{-1}E_A)$, the Joule heat is emitted and a heat exchange with the environment takes place due to the heat removal from the

sample surface. These processes are running with the highest intensity in the case of planar samples. In this case the equation of heat balance for a square cross-section sample with a length of l and a thickness of h is as follows:

$$\rho C(dT/dt) = (jE) - 4\lambda(T - T_0)/h, \quad (12)$$

where λ is coefficient of heat removal from unit area of the sample, C is specific heat capacity and ρ is mass density of the sample (see [1] and [13]), T_0 is ambient temperature.

The Anderson localization emerging at a phase transition (see (7)) results in a feedback between the external electric field and the local magnetization. This is due to the fact that the electric current results in heating of the sample, and thus to an increase in fluctuations of the local magnetization.

The presence of this feedback between current and fluctuations of the local magnetization lays behind the numerical solutions to equation of heat balance (12), which in steady conditions describe the N-shaped current-voltage curves (IU-curves) shown in Fig. 4.

In unsteady conditions ($dT/dt \neq 0$) a self-oscillation of current and local magnetization M_S arises, and in external magnetic fields a self-oscillation of sample magnetization takes place (Fig. 5). And frequency of the self-oscillation increases with increase in the external magnetic field (footnote to Fig. 5). The obtained frequencies of the self-oscillation turn to be one or two orders of magnitude less

than the frequencies used for the measurements of magnetic impedance [15].

6. Conclusion

Thus, in the case of magnetic first-order phase transition in doped manganites a phase with fluctuation short-range order and a semiconductor phase of conduction *s*-electrons emerge in the system of *d*-electrons. The phase immiscibility is accompanied by spatial fluctuations of local magnetization, and the scattering of conduction electrons on them results in the Anderson localization. This transition is realized in the conditions when the chemical potential crosses the region of topological features of the electronic structure and a change in sign of the mode–mode parameter takes place.

Features of the fluctuation-caused phase immiscibility at a first-order phase transition are manifested in external electric and magnetic fields. With a steady self-heating N-shaped IU-curves arise that depend on the external magnetic field. In unsteady conditions not only the self-oscillation of electric current is realized but also the self-oscillation of magnetization takes place, which frequency can be controlled by the external magnetic field.

Further investigation of the self-oscillation of magnetization may be of interest for development of spin current generators based of ferromagnetic semiconductors with CMR.

Funding

The results were obtained as part of the assignment of the Ministry of Science and Higher Education, contract № FEUZ-2023-0015.

Conflict of interest

The authors declare that they have no conflict of interest.

References

- [1] N.G. Bebenin, R.I. Zainullina, V.V. Ustinov, UFN **188**, 8, 801 (2018) (in Russian).
- [2] Yu.A. Izyumov, Yu.N. Skryabin, UFN **171**, 2, 121 (2001) (in Russian).
- [3] N.F. Mott, *Perekhody metall–izolyator*, Nauka, M., (1979), 342 p. (in Russian).
- [4] T. Moria, *Spivoviye fluktuatsii v magnetikakh s kolektivizirovannymi elektronami*, Mir, M., (1988), 288 p. (in Russian).
- [5] M.G. Vergniory, L. Elcoro, C. Felser, N. Regnault, B.A. Bernevig, Z. Wang, *Nature* **566**, 7745, 480 (2019).
- [6] Topological Materials Database: <https://topologicalquantumchemistry.com>
- [7] M. Brando, D. Belitz, F.M. Grosche, T.R. Kirkpatrick. *Rev. Mod. Phys.* **88**, 2, 25006 (2016).
- [8] D.I. Pchelina, V.D. Sedykh, N.I. Chistyakova, V. Rusakov, Y. Alekhina, A. Tselebrovskiy, B. Fraisse, L. Stievano, M.T. Sougrati. *J. Phys. Chem. Sol.* **159**, 110268 (2021).
- [9] K.A. Shaykhtudinov, S.V. Semenov, S.I. Popkov, D.A. Balaev, A.A. Bykov, A.A. Dubrovskiy, N.V. Volkov. *J. Appl. Phys.* **109**, 8, 083711 (2011).
- [10] I.K. Kamilov, K.M. Aliev, K.O. Ibragimov, N.S. Abakarova. *JETP Lett.* **78**, 8, 485 (2003).
- [11] A.A. Abrikosov, L.P. Gorkov, I.E. Dzyaloshinskiy, *Metody kvantovoy teorii polya v statisticheskoy fizike*, Fizmatgiz, M. (1962), 446 p. (in Russian).
- [12] P.W. Anderson. *Local Moments and Localized States: Nobel Lecture*. 8 December (1977).
- [13] P. Lin, S.H. Chun, M.B. Salamon. *J. Appl. Phys.* **87**, 9, 5825 (2000).
- [14] A.A. Povzner, A.G. Volkov. *J. Magn. Magn. Mater.* **432**, 466 (2017).
- [15] G.M.B. Castro, A.R. Rodrigues, F.L.A. Machado, A.E.P. de Araujo, R.F. Jardim, A.K. Nigam. *J. Alloys Compd.* **369**, 108 (2004).

Translated by Y.Alekseev